Published in final edited form as:
*Angew Chem Int Ed Engl*. 2009 ; 48(48): 9097–9101. doi:10.1002/anie.200904504.

# Photochromic Blockers of Voltage-gated Potassium Channels**

**Matthew R. Banghart, Dr.**[†],
Department of Chemistry, University of California Berkeley, Berkeley, California 94720 (USA)

**Alexandre Mourot, Dr.**[†],
Department of Molecular and Cellular Biology, University of California, Berkeley, Berkeley, California 94720 (USA), Fax: (+1) 510 643-6791

**Doris L. Fortin, Dr.**,
Department of Molecular and Cellular Biology, University of California, Berkeley, Berkeley, California 94720 (USA), Fax: (+1) 510 643-6791

**Jennifer Z. Yao**,
Department of Chemistry, University of California Berkeley, Berkeley, California 94720 (USA)

**Richard H. Kramer**, and
Department of Molecular and Cellular Biology, University of California, Berkeley, Berkeley, California 94720 (USA), Fax: (+1) 510 643-6791

**Dirk Trauner, Prof.**
Department of Chemistry, University of California Berkeley, Berkeley, California 94720 (USA); University of Munich, Butenandtstr. 5-13 (F4.086), D-81377 Munich, Germany, Fax: (+49) (0)89 2180-77972

Richard H. Kramer: rhkramer@berkeley.edu; Dirk Trauner: dirk.trauner@cup.uni-muenchen.de

## Keywords

azo compounds; ion channels; photochromism; structure-activity relationships; open-channel block

Photochromic ligands (PCLs) can be optically switched between isomers that show different biological activities. As such, they offer an opportunity to convert ligand-actuated pathways into light-actuated ones, making it possible to control a wide range of biological events with light.

**This work was supported by a Laboratory Directed Research Development Award from the Lawrence Berkeley National Laboratory (R.K.), NSF-DFG grant CHE0724214 (D.T.), the National Institutes of Health Nanomedicine Development Center for the Optical Control of Biological Function (5PN2EY018241) (R.K. and D.T.) and by a grant from the Human Frontier Science Program (RGP23-2005) (R.K. and D.T.). We thank F. Tombola and E. Isacoff for insightful discussion, the Isacoff and Yellen labs for Shaker clones, and T. Fehrentz for experiments not included.

Correspondence to: Richard H. Kramer, rhkramer@berkeley.edu; Dirk Trauner, dirk.trauner@cup.uni-muenchen.de.

[†]These authors contributed equally to this work.

[=]Supporting information for this article is available on the WWW under http://www.angewandte.org or from the author.

PCLs have been explored for various classes of target proteins, including enzymes,[1-3] ligand-gated ion channels,[4-6] and G-protein coupled receptors.[7] For instance, photochromic agonists[5] and antagonists[8] for the nicotinic acetylcholine receptor, a ligand-gated ion channel, have been described more than thirty years ago. More recently, we have introduced a photochromic version of glutamate that acts as a PCL on kainate receptors and can be used to trigger neuronal firing.[6] The PCL approach can be particularly effective in neural networks, whose nonlinear nature can accentuate relatively small changes in efficacy or incomplete photoconversion between isomers.

We now introduce a family of amphiphilic azobenzenes that target tetrameric voltage-gated ion channels (Figure 1a). Channels of this type are not gated by extracellular ligands but can be blocked with small molecules, which are often lipophilic cations.[9, 10] Our molecules function as photochromic blockers of voltage-gated K+ channels and act on the intracellular tetraethylammonium (TEA) binding site (Figure 1b). They can be applied from the extracellular side and have long-lasting effects in cells after a single, transient application. In excitable cells, they function as photochromic neuromodulators and can be used to optically control action potential firing.

One of our molecules, AAQ (**1**), has been previously reported and shown to photosensitize wild-type K+ channels.[11] In our initial publication, we hypothesized that AAQ functions as a photoswitchable tethered ligand (PTL) at the external TEA binding site that would be attached to native residues through affinity labeling (Figure 1c). However, our attempts to verify an interaction at this site were inconclusive (Figures 1 and 2 in the Supporting Information). Instead, our mechanistic studies indicate that AAQ functions in a non-covalenty bound fashion, that is, as a PCL at the internal TEA binding site (Figure 1b).

Potassium channels are not only blocked by alkyl ammonium ions at the external tetraethylammonium (TEA) binding site, but also at the internal entrance to the selectivity filter.[12-15] Charged blockers of the internal but not external TEA binding site, exhibit so called “open-channel block”, wherein pore occupancy does not occur until after the voltage gate has opened.[9, 10, 16] This is most easily observed in Shaker IR (Sh-IR) and other channels lacking the fast-inactivating N-terminal peptide.[17, 18] In response to step depolarization, some ionic current initially flows through unbound channel, but this quickly decays over tens of milliseconds as the blocking molecules bind to the pore.

Figure 2a shows the current responses to depolarizing voltage steps of a HEK293 cell expressing Sh-IR that has been treated with 400 μM AAQ. Under 380 nm irradiation, channels are not blocked by AAQ (gray trace). However, when channels are blocked by AAQ with 500 nm light, an initial transient current remains ($I_{pk}$), which rapidly decays so that nearly all of the steady-state current ($I_{ss}$) is blocked (black trace). This effect is not observed during blockade of SPARK channels,[19] which contain an extracellular cysteine for covalent attachment of the maleimide analogue MAQ (**2**) (Figure 2b).

These data suggest that AAQ acts predominantly at the internal TEA binding site of Sh-IR, while MAQ acts on the external TEA binding site of SPARK channels.[20, 21] A more extensive characterization of the open-channel block observed with AAQ is provided in

Figure 3 of the Supporting Information. These experiments directly demonstrate the requirement for channel opening to occur before AAQ is able to block the pore and reveal that pore occupancy is correlated with the frequency of channel opening.

Further indicating the internal TEA binding site, the current *versus* voltage (I/V) curve shows that block by AAQ is distinctly voltage-dependent, such that $I_{ss}$ is blocked more effectively at more depolarized membrane potentials (Figure 2c). Under 380 nm illumination, the current increases linearly with voltage once the channels are fully activated (gray line). At 500 nm, current is predominantly blocked at all membrane potentials (black line). However, 420 nm, which produces only partial conversion to *cis* isomer, reveals voltage-dependent block (dashed black line), as indicated by the decline in $I_{ss}$ at potentials more positive than + 10 mV (Figure 4a in the Supporting Information shows the raw current responses). This is typical of positively charged intracellular K+ channel blockers.[10, 22] Just as depolarization provides a driving force for positively charged K+ ions to flow in the outward direction, internal alkyl ammonium ions are driven into their binding site within the membrane electric field and block more effectively as membrane depolarization is increased.

Because ions move single file through the permeation pathway of K+ channels, high concentrations of external K+ ($[K+]_o$) electrostatically repel intracellular charged blockers to accelerate their exit rate from the channel and thereby reduce their blocking potency.[23, 24] Accordingly, the extent of AAQ block correlates inversely with the extracellular potassium concentration $[K+]_o$, as revealed by the currents shown in Figure 2d. After establishing voltage clamp in standard external buffer ($[K+]_o$ = 1.5 mM) and measuring $I_{ss}$ under 380 and 500 nm light, cells were locally perfused with solutions containing 0.3 mM and 20 mM $[K+]_o$. We controlled for the change in maximal current resulting from the altered K+ driving force by measuring currents at 380 nm, which completely unblocks the channels. This trend was consistent across the range of voltages that activate Sh-IR (Figure S4b of the Supporting Information).

Consistent with this mode of action, direct application of AAQ to the internal TEA binding site in both inside-out patch (Figure 3) and whole cell recordings (Figure 5a of the Supporting Information) also produced photoswitchable open-channel block. Because inclusion in the patch pipette does not permit solution exchange at the cytosolic interface, inside-out patches were pulled from HEK293 cells expressing Sh-IR to allow AAQ application followed by washout. In this case, current block by AAQ was relieved within several seconds of washout (Figure 3a), indicating that covalent reaction did not occur under these conditions. Dose-response curves could therefore be generated by illuminating patches with 380 and 500 nm light in the presence of different concentrations of AAQ. Summary data for photostationary states enriched in *trans*- and *cis*-AAQ are shown in Figure 3b, which reveal a 30-fold difference in blocking potency (500nm $IC_{50}$ = 2.0 μM ± 0.2 μM, 380nm $IC_{50}$ = 64 μM ± 2.1 μM, *n* = 3-5). Because photoswitchable block was observed without any indication of covalent modification, these experiments demonstrate that AAQ can block as a PCL at the internal TEA binding site.

As an acrylamide, AAQ contains an electrophilic functional group, yet our data indicated that analogues lacking an electrophile would function in a similar manner. To test this model and identify photochromic blockers with improved biophysical properties, we prepared a series of analogues (Figure 1a, **3**-**10**). To facilitate partitioning into the membrane, several analogues contain aliphatic "tails" of increasing hydrophobicity (**3**-**7**). By contrast, the doubly charged, symmetric analogue **8** was expected to exhibit poor membrane penetration. In other members of the series, the amide "tail" was either removed completely (**9**) or replaced with a propyl group (**10**) to mimic the length of **3**, the shortest amide examined. Prior to screening, UV/Vis spectroscopy confirmed that 380 nm and 500 nm light produced nearly identical photostationary states for each compound, consisting of at least 80% *cis* and *trans* isomers respectively (data not shown). (Chemical synthesis is available in the Supporting Information)

Strikingly, after a brief extracellular application followed by washout, all of the new compounds containing a hydrophobic tail (**3-7, 9, 10**) were found to function as open-channel blockers and persistently blocked Sh-IR currents for the duration of a typical recording (5 min). $I_{ss}$-recordings under repeated 380 nm and 500 nm illumination from cells treated with either AAQ, **7** or **10** are shown in Figure 4a-c, and step responses to depolarization for each new compound are shown in Figure 5b-i of the Supporting Information.

A general trend was observed in which potency is correlated with tail length and hydrophobicity, represented in Table 1 as the lowest concentration producing >95% block of $I_{ss}$ at +40 mV. The doubly charged analogue **8** did not block channels after extracellular treatment (tested at concentrations up to 2 mM), although inclusion in the patch pipette did afford photoswitchable block (not shown). Compound **7**, named Benzoyl-Azo-QA (BzAQ), was found to block >95% of $I_{ss}$ at only 25 μM. A dose-response curve obtained from inside-out patches (Figure 4d) indicates that *trans*-BzAQ has a similar affinity to *trans*-AAQ when applied directly to the internal TEA binding site (500 nm $IC_{50}$ = 1.3 μM ± 0.2 μM, 380 nm $IC_{50}$ = 83 μM ± 20 μM, $n$ = 4). Therefore, its enhanced potency is most likely due to better membrane partitioning rather than increased affinity for the blocking site.

In contrast to the amides **3-7,** compound **9** exhibited comparable block in both *cis* and *trans* forms (in the Supporting Information). This suggests that interactions between the "tail" and channel protein might account for the differences in affinity between isomers. Indeed, compound **10**, named Propyl-Azo-QA (PrAQ), preferentially blocks in the *cis* form (Figure 4c). External treatment with 40 μM of compound **10** provided ∼50% block of $I_{ss}$ in the *cis* form without producing obvious block by the *trans* isomer as judged by the lack of rapid current decay at 500 nm. However at higher concentrations, blockade by the *trans* isomer was apparent (data not shown). Because the thermally stable *trans*-isomer is inactive, optimized *cis*-blocking analogues of PrAQ will reduce cellular exposure to UV-light and avoid unintentional channel blockade during PCL application in the dark.

To determine if these novel PCLs function like AAQ in neurons, we examined the most potent analogue, BzAQ (**7)** in dissociated hippocampal cultures, a preparation in which AAQ was previously found to photosensitize endogenous K+ after preincubation at 300

μM.[11] Current-voltage curves from neurons recorded in whole-cell voltage clamp showed that the K+ channels contributing to $I_{ss}$ in neurons are modulated after extracellular treatment with 20 μM BzAQ (Figure 5a). From this data, $I_{ss}$ at +40 mV was compared at 380 and 500 nm, revealing that on average, 35.5% ± 4.7% ($n$ = 10) of $I_{ss}$ is blocked by BzAQ under these conditions. In current clamp mode, which allows the recording of action potentials, BzAQ was found to depolarize the cellular membrane potential when switched from *cis* to *trans*, which was sufficient to induce action potential firing (Figure 5b). Furthermore, BzAQ did not affect depolarizing Na+ currents in neurons (not shown) and did not photosensitize voltage-gated Na+ or Ca2+ channels expressed in GH3 cells (Figure 6 in the Supporting Information), like AAQ.[11] Together, these data indicate that BzAQ is an effective photomodulator of neural activity with features similar to AAQ,[11] but with the advantage of increased potency, while avoiding the potential toxicity and immunogenicity associated with reactive reagents.

The results presented here do not explain how these molecules are retained by cells for long periods of time. While AAQ can effectively photosensitize Sh-IR in HEK293T cells for just longer than one hour, dissociated hippocampal neurons respond to light at least 24 hours after exposure to AAQ (Figure 7 in the Supporting Information). It is likely that retention occurs by tight association with the plasma membrane, as is the case with a structurally related styryl-class of fluorophores, which includes the endosomal marker FM1-43[25] and many voltage sensitive dyes.[26] Consistent with this, classic local anesthetics have been proposed to access the internal binding site of voltage-gated sodium channels through hydrophobic pathways.[27] Regardless of the exact mechanism of retention, the phenomenon of long-lasting block is not unique to our photochromic blockers. An array of hydrophobic ammonium ions such as the lidocaine derivative Tonocaine, and tetrapentylammonium (TPeA), have been show to get trapped after crossing the cell membrane to block voltage-gated sodium and potassium channels for many minutes after washout.[28, 29]

AAQ was designed to act covalently at the external TEA binding site. Although the results presented here do not rule out covalent modification of Sh-IR altogether, they do suggest that it predominantly acts as a PCL at the internal TEA binding site instead. This has allowed us to define an entire class of photochromic ligands that have a new mode of function and explore their structure-activity relationships in detail. Given the many structural, functional and pharmacological similarities of voltage-gated ion channels, the principles established herein should also enable the development of additional PCLs for voltage-gated Na+ and Ca2+ channels. Our photochromic neuromodulators have already proven themselves as useful tools in neurobiology and could have therapeutic value, for instance in attempts to restore vision.

## Supplementary Material

Refer to Web version on PubMed Central for supplementary material.

## References

1. Kaufman H, Vratsanos SM, Erlanger BF. Science. 1968; 162:1487–1489. [PubMed: 5700068]
2. Wainberg MA, Erlanger BF. Biochemistry. 1971; 10:3816–3819. [PubMed: 5160410]

3. Harvey AJ, Abell AD. Tetrahedron. 2000; 56:9763–9771.
4. Deal WJ Jr, Erlanger BF, Nachmansohn D. Proc Natl Acad Sci USA. 1969; 64:1230–1234. [PubMed: 5271749]
5. Bartels E, Wassermann NH, Erlanger BF. Proc Natl Acad Sci USA. 1971; 68:1820–1823. [PubMed: 5288770]
6. Volgraf M, Gorostiza P, Szobota S, Helix MR, Isacoff EY, Trauner D. J Am Chem Soc. 2007; 129:260–261. [PubMed: 17212390]
7. Nargeot J, Lester HA, Birdsall NJ, Stockton J, Wassermann NH, Erlanger BF. J Gen Physiol. 1982; 79:657–678. [PubMed: 6978380]
8. Krouse ME, Lester HA, Wassermann NH, Erlanger BF. J Gen Physiol. 1985; 86:235–256. [PubMed: 4045419]
9. Armstrong CM. J Gen Physiol. 1969; 54:553–575. [PubMed: 5346528]
10. French RJ, Shoukimas JJ. Biophys J. 1981; 34:271–291. [PubMed: 7236852]
11. Fortin DL, Banghart MR, Dunn TW, Borges K, Wagenaar DA, Gaudry Q, Karakossian MH, Otis TS, Kristan WB, Trauner D, Kramer RH. Nat Methods. 2008; 5:331–338. [PubMed: 18311146]
12. Armstrong CM, Binstock L. J Gen Physiol. 1965; 48:859–872. [PubMed: 14324992]
13. Armstrong CM. Nature. 1968; 219:1262–1263. [PubMed: 5677423]
14. Choi KL, Mossman C, Aube J, Yellen G. Neuron. 1993; 10:523–531. [PubMed: 8461139]
15. Zhou M, Morais-Cabral JH, Mann S, MacKinnon R. Nature. 2001; 411:657–661. [PubMed: 11395760]
16. Hille, B. Ion Channels of Excitable Membranes. 3rd. Sinauer; Sunderland, MA: 2001.
17. Yellen G, Jurman ME, Abramson T, MacKinnon R. Science. 1991; 251:939–942. [PubMed: 2000494]
18. Hoshi T, Zagotta WN, Aldrich RW. Science. 1990; 250:533–538. [PubMed: 2122519]
19. Banghart M, Borges K, Isacoff E, Trauner D, Kramer RH. Nat Neurosci. 2004; 7:1381–1386. [PubMed: 15558062]
20. MacKinnon R, Yellen G. Science. 1990; 250:276–279. [PubMed: 2218530]
21. Blaustein RO, Cole PA, Williams C, Miller C. Nature Struct Biol. 2000; 7:309–311. [PubMed: 10742176]
22. Armstrong CM. J Gen Physiol. 1971; 58:413–437. [PubMed: 5112659]
23. Armstrong CM. J Gen Physiol. 1966; 50:491–503. [PubMed: 11526842]
24. Demo SD, Yellen G. Neuron. 1991; 7:743–753. [PubMed: 1742023]
25. Zhu Y, Stevens CF. Proc Natl Acad Sci USA. 2008; 105:18018–18022. [PubMed: 19004790]
26. Zecevic D, Djurisic M, Cohen LB, Antic S, Wachowiak M, Falk CX, Zochowski MR. Curr Protoc Neurosci. 2003 Unit 6.17.
27. Hille B. J Gen Physiol. 1977; 69:497–515. [PubMed: 300786]
28. Wang GK, Quan C, Vladimirov M, Mok WM, Thalhammer JG. Anesthesiology. 1995; 83:1293–1301. [PubMed: 8533922]
29. Taglialatela M, Vandongen AMJ, Drewe JA, Joho RH, Brown AM, Kirsch GE. Mol Pharmacol. 1991; 40:299–307. [PubMed: 1875913]

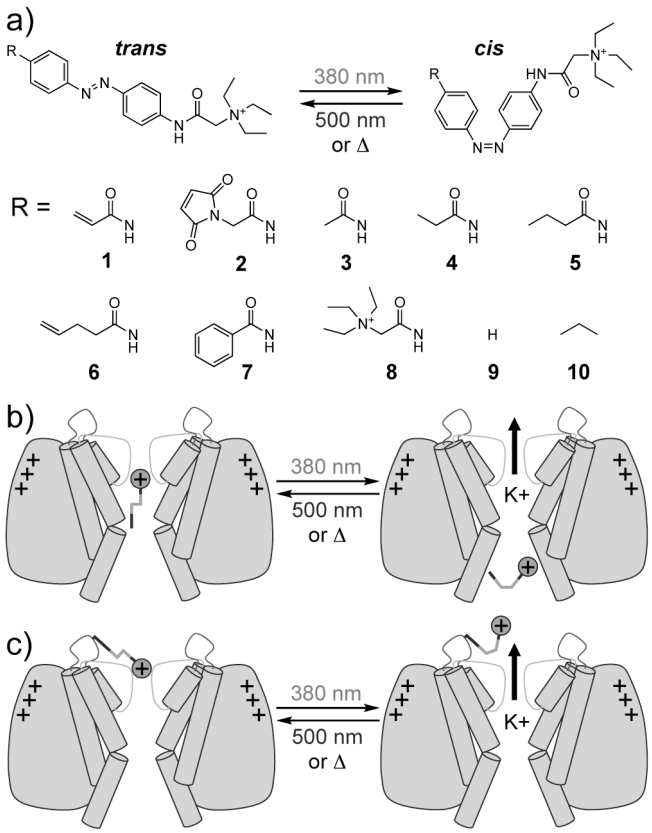


**Figure 1.**

Photocontrol of K+ channels. a) Structures and photoisomerization of photoswitchable K+ channel blockers. b) Cartoon depicting a PCL for the internal TEA-binding site. The linear *trans* isomer is a better blocker than the bent *cis* isomer. c) Cartoon depicting a PTL for the external TEA-binding site. The extended *trans* isomer presents the blocking particle to the pore while the shorter *cis* isomer is unable to reach. PCL: photochromic ligand, PTL: photoswitchable tethered ligand, TEA: tetraethylammonium.

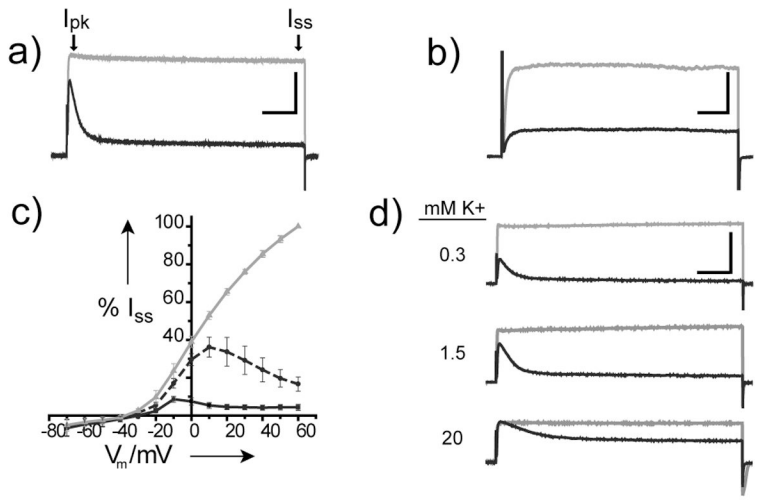


**Figure 2.**

AAQ is an open-channel blocker of the Sh-IR internal TEA-binding site. *a* & *b*) Whole-cell current responses to 200 ms depolarizing voltage steps from −70 to +40 mV in the presence of 380 nm (gray) or 500 nm (black) light. *a*) Open-channel block is apparent in AAQ-treated Sh-IR channels (Scale bar: 6 nA, 25 ms.) *b*) Open-channel block is absent in MAQ-treated SPARK channels (Scale bar: 0.5 nA, 25 ms.) *c*) Steady-state I/V curves under 380 nm (gray), 420 nm (black dashes) and 500 nm (black) illumination. I/V curves from each of 4 cells were normalized to the current measured at 380 nm and +60 mV. *d*) Dependence of AAQ block on $[K+]_o$. Whole-cell current responses of a cell to depolarizing voltage steps from –70 to +40 mV in the presence of 380 nm (gray) or 500 nm (black) light at the indicated $[K+]_o$. Similar results were obtained in 2 other cells (Scale bar: 5 nA, 50 ms.)

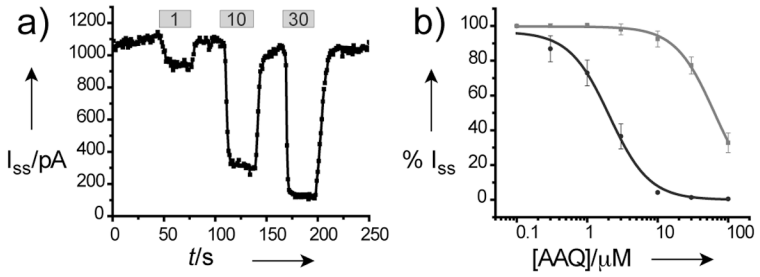


**Figure 3.**

AAQ is a PCL for the internal-TEA binding site of Sh-IR. (*a*) $I_{ss}$ recorded from inside-out patches as AAQ was applied at the indicated concentrations (μM). (*b*) Dose-response relationships for AAQ applied to inside-out patches under 500 nm (black) and 380 nm (gray) illumination.

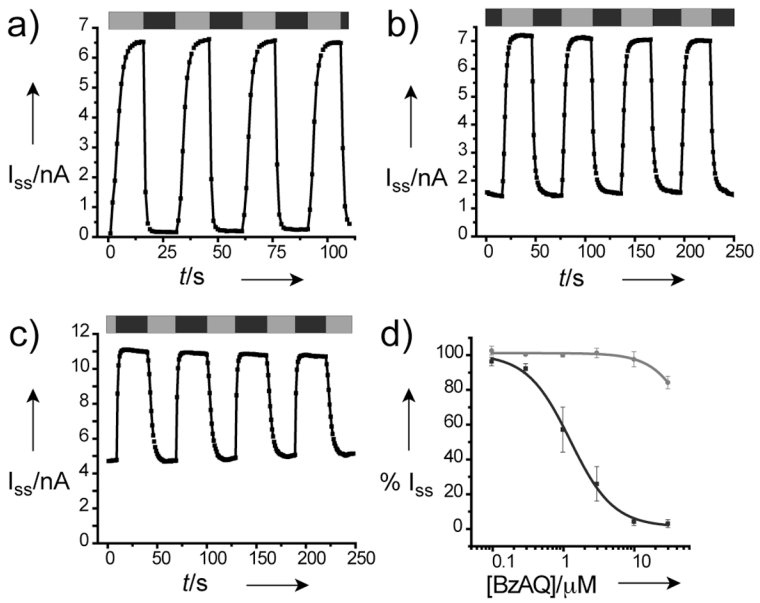


**Figure 4.**

PCLs persistently photosensitize Sh-IR. $I_{ss}$ over time recorded from a cell treated with a) 400 μM AAQ, *b*) 20 μM BzAQ (**7**) and *c*) 40 μM PrAQ (**10**) under 380 nm (gray bars) and 500 nm (black bars) illumination. *d*) Dose-response relationships for BzAQ (**7**) applied to inside-out patches under 500 nm (black) and 380 nm (gray) illumination.

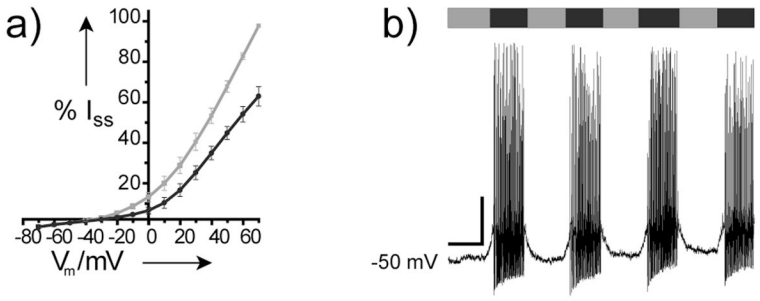


**Figure 5.**

BzAQ photoregulates endogenous K+ channels in dissociated hippocampal neurons to modulate neural activity. *a*) Steady-state I/V curves under 380 nm (gray) and 500 nm (black) illumination recorded from neurons treated with 20 μM BzAQ. Recordings from 4 individual cells were normalized to the current measured at 380 nm and +70 mV. *b)* Current clamp recording from a neuron showing the induction of action potential firing in response to 500 nm light (black). Scale bar: 10 mV, 10 s. Similar results were obtained in at least 3 additional cells.

## Table 1

### Structure-Activity Relationships

| Compound | μM[a] | % Block[b] | Active Isomer |
|---|---|---|---|
| **1** (AAQ) | 400 | >95 | *trans* |
| **2** (MAQ) | 400[c] | 0 | - |
| **3** | 1000 | >95 | *trans* |
| **4** | 800 | >95 | *trans* |
| **5** | 300 | >95 | *trans* |
| **6** | 200 | >95 | *trans* |
| **7** (BzAQ) | 25 | >95 | *trans* |
| **8** | 2000 | 0 | *trans* |
| **9** | 1000 | ND[d] | *trans = cis* |
| **10** (PrAQ) | 40 | ~50 | *cis* |

[a] Concentrations reported for **1-6** & **8** were determined by first identifying a dose producing >95% block. We then reduced the concentration in 100 μM increments until <95% block was observed. For compounds **7** and **10**, 5 μM increments identified the reported values. At each reported concentration, determinations were repeated in 3-5 cells from two separately treated coverslips.

[b] For compounds **1-9**, % Block was calculated as the % of $I_{SS}$ measured at 380 nm that was blocked at 500 nm. For compound **10**, the wavelengths were reversed. In each case, unblock was estimated as complete by the lack of open-channel block, as shown in Figure 5 of the Supporting Information.

[c] Treatment of HEK293 cells with MAQ at concentrations >400 μM did not afford stable recordings.

[d] Although substantial open-channel block was observed, the lack of unblock at either wavelength prevented calculation of % Block.